



Tokamak Divertor Impact on the Toroidal Field Magnet and Vacuum System

Y. Gohar and C.W. Maynard

October 1977

UWFDM-222

***FUSION TECHNOLOGY INSTITUTE
UNIVERSITY OF WISCONSIN
MADISON WISCONSIN***

Tokamak Divertor Impact on the Toroidal Field Magnet and Vacuum System

Y. Gohar and C.W. Maynard

Fusion Technology Institute
University of Wisconsin
1500 Engineering Drive
Madison, WI 53706

<http://fti.neep.wisc.edu>

October 1977

UWFDM-222

TOKAMAK DIVERTOR IMPACT ON THE TOROIDAL FIELD MAGNET AND
VACUUM SYSTEM

Y. Gohar
Argonne National Laboratory
Argonne, Illinois 60439

and

C. W. Maynard
University of Wisconsin
Madison, Wisconsin 53706

Neutronic analysis for the Wisconsin Tokamak Engineering Test Reactor (TETR) blanket/shield design has been carried out in detail for the different sections of the reactor (test section, outer blanket, inner blanket, neutral beam injectors and the divertor). Special attention has been given to the divertor shield design since the divertor is one of the most difficult components of the reactor to design. The divertor slots represent a source of neutron leakage which requires careful analysis of the actual geometry and shield to minimize the effects on the reactor. The toroidal-field (TF) magnet is the most sensitive component that suffers from the divertor concept. The radiation leakage from the divertor increases the copper resistivity, the nuclear heating and causes degradation in the insulator properties. The other effects caused by the radiation leakage are the nuclear heating in the cryosorption panel and the increase in the radiation dose outside the reactor shield. Multidimensional neutronics calculations are used for the analysis of these effects with iteration on the divertor geometry to satisfy the following design criteria: (1) the maximum degradation in the insulator properties is 30% at 15 MW-yr/m^2 integrated neutron wall loading, (2) the maximum change in the copper resistivity is 50% at any point in a TF magnet at a 3.5 MW-yr/m^2 integrated neutron wall loading, (3) the heat deposition in the TF magnet is $< 60 \text{ KW(th)}$, and (4) the maximum nuclear heat load for the cryosorption panels is $< 0.001 \text{ W/cm}^3$ to minimize the refrigeration power. It is found that the maximum damage in a TF magnet is located near the divertor area. The ratio of the maximum change in the copper resistivity to the change in the resistivity at the midplane of the reactor (where the design is usually carried out) is about 9. The heat deposition in the cryosorption panel is reduced by two orders of magnitude by using a special shield for the vacuum system which reduces the initial and the operational costs. The refrigeration power and the dose to the insulator satisfy the design requirements after an iteration on the divertor geometry and its shield.

INTRODUCTION

The fusion community has proposed various Tokamak reactor designs which can be classified into two different categories, the experimental devices and the power reactors. At first glance, one can characterize the power reactors by a long burn cycle and a divertor concept (although some of the experimental devices utilize the divertor concept). The Tokamak fusion reactors employ the divertor concept to reduce the erosion of the first wall due to energetic charged particle bombardment and to protect the plasma from high Z impurities as is essential to achieve a long burn cycle. Various types of divertors have been proposed¹, single null, double null, and bundle. The different types require a large opening (divertor slots) in the blanket/shield for particle collection. The TETR divertor design has been carried out in detail to illustrate and minimize the divertor impact on the reactor. In particular the effects on the toroidal field (TF) magnets and the vacuum system since these two subsystems suffer greatly from the divertor concept.

The TETR design parameters required for this paper are given in Table 1 and a cross sectional view of the TETR reactor is shown in Figure 1. The TETR has been designed to be a mid-term experimental device² to provide engineering data for the fusion power program. This objective lead us to consider the existing state of the art without extrapolation for the design. The reactor chamber of TETR is designed for 1 MW/m^2 average neutron wall loading to get the required data in a reasonable timeframe for the fusion program. The TF magnets are "D" shaped superconducting coils. The conductor consists of NbTi filaments with OFHC copper stabilizer using stainless steel as the structural material. Cryosorption panels are used in the vacuum system.

DESIGN CONSTRAINTS

The design philosophy for TETR requires the achievement of an integrated neutron wall loading of 15 MW/m^2 within 15 years of operation ($1.4 \text{ MW/m}^2/\text{yr}$ neutron wall loading with a plant factor of 0.7). The requirement of operation for 15 years with 70% plant factor imposes many design constraints which are used in this work.

The TF magnets are designed to operate without replacement for 15 years, but under the expected radiation environment the material properties will be degraded. The TF magnets consist of superconducting material (NbTi) embedded in copper (the stabilizer) using stainless steel as the structural material. Two insulator materials are used, epoxy as an electrical insulator and mylar as a thermal insulator. The neutron flux environment reduces the critical temperature (T_c) and the critical current (J_c) for the superconductor. The change in T_c is very small and can be neglected. On the other hand the change in the critical current affects the superconductor size required to carry the same current after irradiation. The experimental study by Soel⁵ shows a 10% reduction in the critical current when the conductor receives a neutron dose of $3 \times 10^{18} \text{ n/cm}^2$. This reduction in the critical current can be accommodated during the design stage or by use of the annealing process every few years of operation. The experimental data⁵ shows the annealing process at 300° K restores the critical current to 98% of the value before the irradiation. The TETR toroidal field magnets are designed to require annealing every five years of operation. This requires a 4% increase in the conductor size to accommodate the reduction in the critical current after 5 years of operation.

The resistivity of the normal conductor (stabilizer) is more sensitive to the neutron dose¹ at low temperature. The increase in the copper resis-

tivity is about 13 times the original value following irradiation to the 10^{-3} dpa damage level. This implies that the change in copper resistivity cannot be accommodated during the design process. The design criterion for TETR is to allow a maximum 50% increase in the copper resistivity after 5 years of operation since the experimental data⁹ show the annealing process at room temperature restores most of the original value of the resistivity (80% recovery for copper). Further, the annealing process at 77°K every few years is considered as a possibility for TETR. With these operational plans, the copper stabilizer is designed for a 50% increase in the copper resistivity.

Radiation damage to the insulators is more serious, since there is no way to restore the degradation in mechanical properties. The useful radiation limit is about 10^{17} n/cm² (1.2×10^8 rads) and 10^{19} n/cm² (10^{10} rads) for mylar and epoxy respectively. The organic material can be combined with inorganic reinforcement to increase the limit to 10^{18} n/cm² (10^9 rads).

The blanket/shield is designed to minimize the energy deposition in the TF magnets since each watt deposited at 4°K requires about 300 to 500 watts of refrigeration power.

The last constraint is related to the heat deposited in the cryosorption panels by neutron and gamma interactions. The panels are designed for a 0.001 w/cm^3 maximum heat load at the panel surface due to these interactions to limit the refrigeration power.

CALCULATIONAL MODEL

The large opening (divertor slots) used for the divertor represent a source of neutron and gamma leakage which affects the vacuum system and the TF magnets. In addition, these slots occupy a significant amount of space

which would otherwise shield the inner leg of the TF magnets. The usual one dimensional model was used for calculations based on an infinite cylinder resulting from a vertical cut through the torus. This model is acceptable for a system which has poloidal symmetry, a centered plasma, and a high aspect ratio. Another model which accounts for an off-center plasma and a low aspect ratio is based on an infinite cylinder resulting from a horizontal cut through the torus at the midplane. This model was developed for UWMAK-III⁶ and used for TETR to obtain the midplane results. In general these one dimensional models can be used for a parametric study at an early stage in the design, but it is unrealistic to use such models for detailed information. Finally, a two dimensional R-Z geometry model was used to represent the actual geometric details as shown in Figure 1.

The parametric study for TETR³ shows clearly that a heavy material must be used for the blanket/shield to satisfy the design constraints and to minimize the operating cost. A combination of tungsten, stainless steel, lead, and boron carbide gives the best performance and minimum radioactivity and dose outside the reactor³, which reduces the maintenance costs. Stainless steel has been chosen as a structural material for TETR; the basis for the choice is the available data about this material with a minimum extrapolation for the fusion environment.

The calculations employ a neutron cross section data set of 46 energy groups based on DLC-37 with the P_3 approximation. A modified version of the DOT program⁸ was used to perform the calculations in the S_6 approximation.

RESULTS

First, blanket/shield calculations have been executed based on 1-D transport model at the midplane. These calculations determined the

shielding composition and thickness.³ Then a detailed 2-D toroidal transport calculation using the actual geometry shown in Figure 1 and the neutron source distribution over space was carried out. The results from the 1-D calculations at the midplane satisfy the design criteria. A sample of the results from the 1-D calculations and the corresponding results from 2-D calculations are given in Table 2. The comparison between the 1-D and 2-D results at the midplane shows the 1-D model underestimates the integral quantities by a factor of 4 to 6. In fact, these differences are expected because the 2-D model considers a finite source and toroidal geometry compared to the 1-D model which considers an infinite cylinder geometry and source distribution.

Figure 2 shows the neutron flux ($E > 0.1$ MeV) in the divertor area where the magnet receives a maximum dose at 2.0 meters above the midplane. The magnet receives a maximum dose of 1.2×10^{10} n/cm² sec compared to 3.4×10^9 at the midplane and 2.3×10^9 from the 1-D calculations at $R = 1.6$ meters. The average dose results in a 1.0% decrease in the critical current after 5 years of operation. This reduction in the critical current is accounted for during the design stage. The average displacement rate in the copper conductor satisfies the design criterion, but the displacement rate in the first ten centimeters facing the plasma is relatively high as shown in Figure 3. A combination of two different approaches is considered to accommodate the change in the copper resistivity. The first approach is to design the copper conductor to accommodate a change in the resistivity greater than the average in this area. The second approach is to warm the magnet to reduce the copper resistivity.⁹ The actual criterion is to operate the magnet with a heat flux less than 0.4 watt/cm² when all the current is passing through the copper conductor.

The heat deposition rate in the toroidal field magnet is plotted in Figure 4. This shows a maximum of 0.0003 watt/cm^3 which is quite satisfactory. The maximum dose in mylar exceeds the maximum allowable by a factor of five which means another insulation material must be used in the area where the maximum dose exceeds the limit. On the other hand the maximum dose for the epoxy is much less than the limit as can be seen from inspection of Figure 2.

Figure 5 shows the neutron and gamma heat deposition rate in the cryosorption panels. The panels are designed for 0.1 watt/cm^3 maximum heat load which means the nuclear heating limit is of the order of 0.001 watt/cm^3 . The maximum neutron and gamma heating rate from Figure 5 is about $0.00007 \text{ watt/cm}^3$ which satisfies the design requirement. This low heating rate is achieved by using a shadow shield (chevron shield) in front of the cryosorption panels.

CONCLUSIONS

This nuclear analysis of a tokamak reactor employing the divertor concept points out the following important results. It is found that:

1. The maximum damage in the toroidal field magnets is located in the divertor area.
2. The organic insulators require a factor 5 to 10 improvement in the maximum allowable dose while the inorganic insulators appear to be quite satisfactory.
3. The increase in the electrical resistivity of the stabilizer requires the toroidal field magnets to be warmed periodically for annealing. This process effects the availability of the reactor but lowers the magnet cost.

4. The one dimensional analysis represents an underestimate of the integral quantities for the toroidal field magnets by an order of magnitude.

REFERENCES

1. B. Badger, et al., "A Wisconsin Toroidal Fusion Reactor Design -- UWMAK-I," UWFD-68 Univ. of Wisconsin (1976).
2. G. L. Kulcinski, et al. "TETR -- A Tokamak Engineering Test Reactor to Qualify Materials and Blanket Components for Early DT Fusion Power Reactors," UWFD-173, Univ. of Wisconsin (1976).
3. G. L. Kulcinski, et al., "A Near Term Tokamak Engineering and Materials Test Reactor -- TETR," UWFD-191, Univ. of Wisconsin (1977).
4. R. W. Conn, Y. Gohar, and C. W. Maynard, Transactions American Nuclear Society, 23, 12, (1976).
5. M. Soel, "The Influence of Radiation Damage on the Properties of a Superconductor," IPP 4/104, Max Planck Institut (1972).
6. Y. Gohar, C. W. Maynard, and E. T. Cheng, "Neutronic and Photonic Analysis of UWMAK-III Blanket and Shield in Non Circular Toroidal Geometry," published in Proceedings of the 2nd ANS Topical Meeting on the Technology of Controlled Nuclear Fusion, Richland, Washington (September 21-23, 1976).
7. D. M. Plaster, R. T. Santoro, and W. E. Ford III, "Coupled 100 Group Neutron and 21 Group Cross Section for EPR Calculations," ORNL-TM-4872, Oak Ridge National Laboratory (1975).
8. W. A. Rhoads, F. R. Mynatt, "The Dot-III Two Dimensional Transport Code," ORNL-TM-4280, Oak Ridge National Laboratory (1975).
9. J. A. Horak, and T. H. Blewitt, "Isochronal Recovery of Fast Neutron Irradiated Metals," Journal of Nuclear Materials 49(1973/74) 161-180.

Table 1 -- TETR Design Parameters

Fuel Cycle	D-T
Burn Time	60 sec
Total Cycle Time	72.5 sec
Major Radius	3.25 m
Impurity Control	Double Null Divertor
TF Superconductor	NbTi
Number of TF Coils	16
Magnet Insulation	Micarta, Epoxy, Fiberglass
Magnet Stabilizer	OFHC Copper
Magnet Structure	316 SS
Conductor Current	9838 A
Thermal Power Output	346 MW
Average Neutron Wall Loading	1 Mw/m ² /yr
Basic Structure	316 SS

Table 2 -- 1-D and 2-D Results Compared at the Midplane
to the Design Constraints

	<u>Design Requirement</u>	<u>1-D</u>	<u>2-D</u>
Neutron flux at R = 160 cm E > 0.1	--	7.2×10^8	3.4×10^9
Neutron flux at R = 160 cm E > 0.0	--	2.3×10^9	9.3×10^9
Maximum displacement rate in Cu at R = 160 cm dpa/YR	--	1.2×10^{-5}	5.5×10^{-5}
Average displacement rate in Cu dpa/YR	4×10^{-5}	1.2×10^{-6}	7.0×10^{-6}
Maximum dose in Mylar n/cm ²	10^{18} (10^9 rads)	1.2×10^{18} (1.95×10^8 rads)	4.74×10^{18}
Maximum heat load in the TF magnets w/cm ³	0.01	5.0×10^{-5}	3.0×10^{-4}

Figure (1) Cross Section View of the TETR Reactor

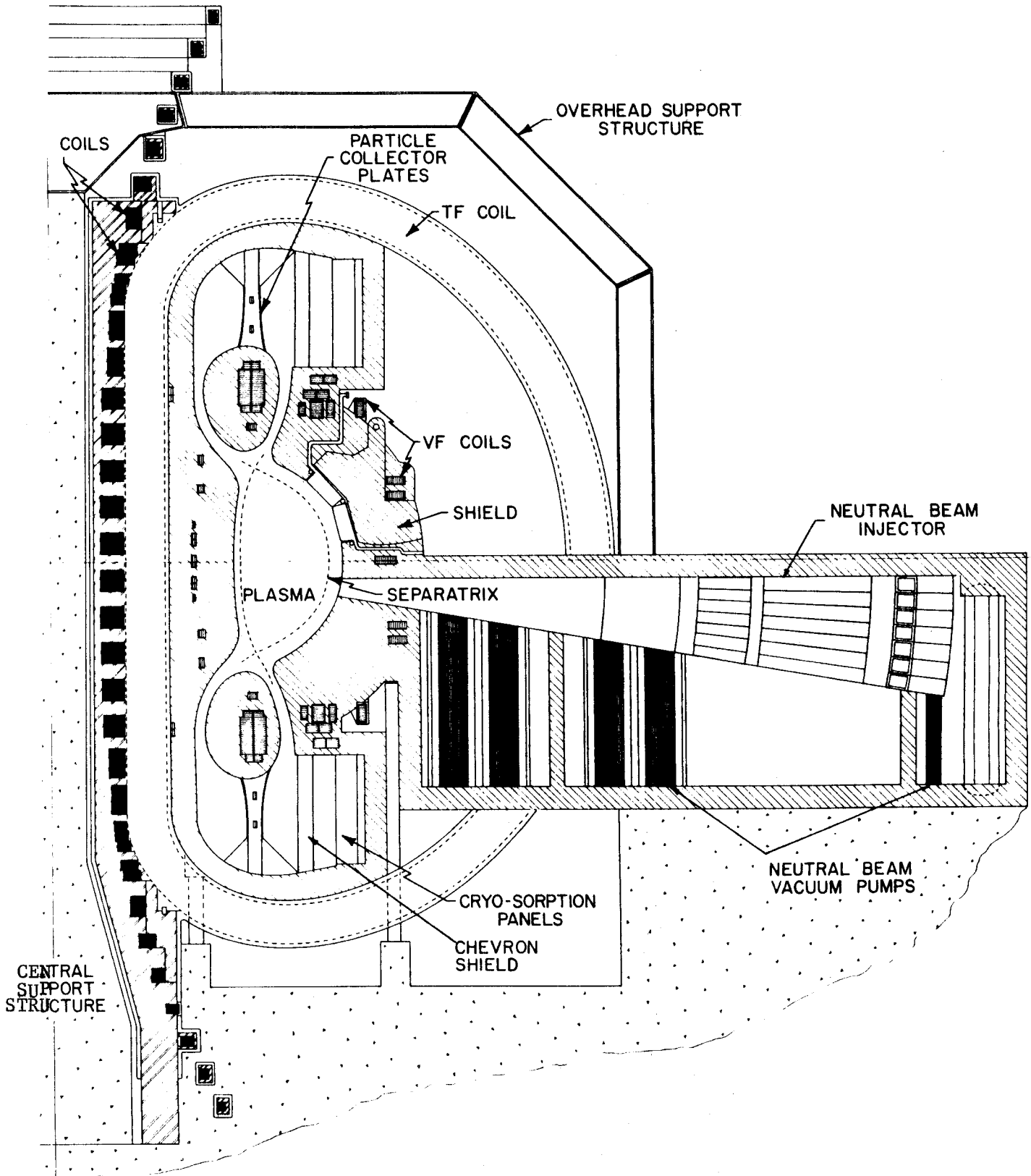


Figure (2) The Neutron Flux ($E > 0.1$ MeV) in the Divertor Area

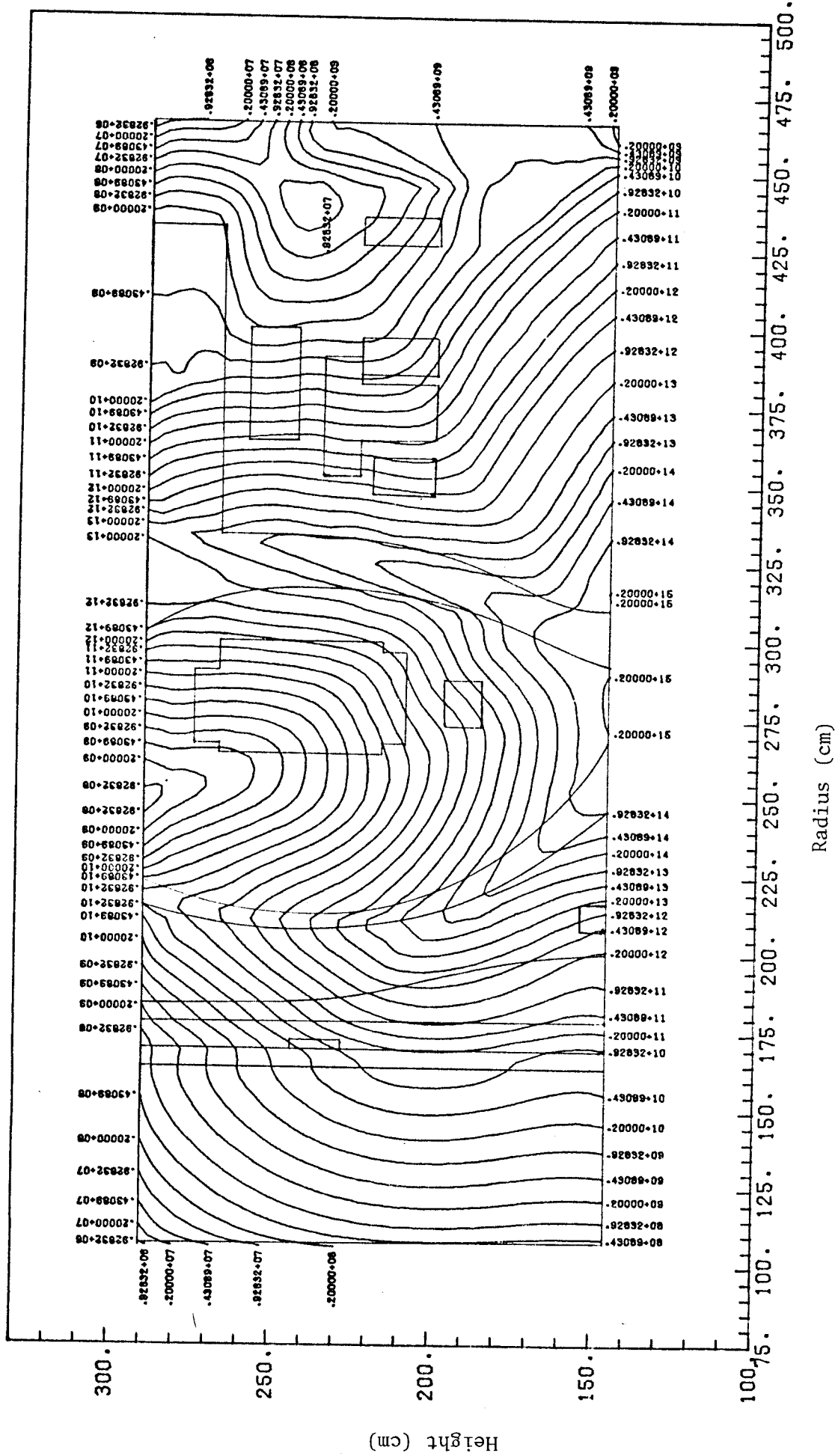


FIGURE (3) ATOMIC DISPLACEMENT RATE IN THE COPPER CONDUCTOR (DPA/YEAR)

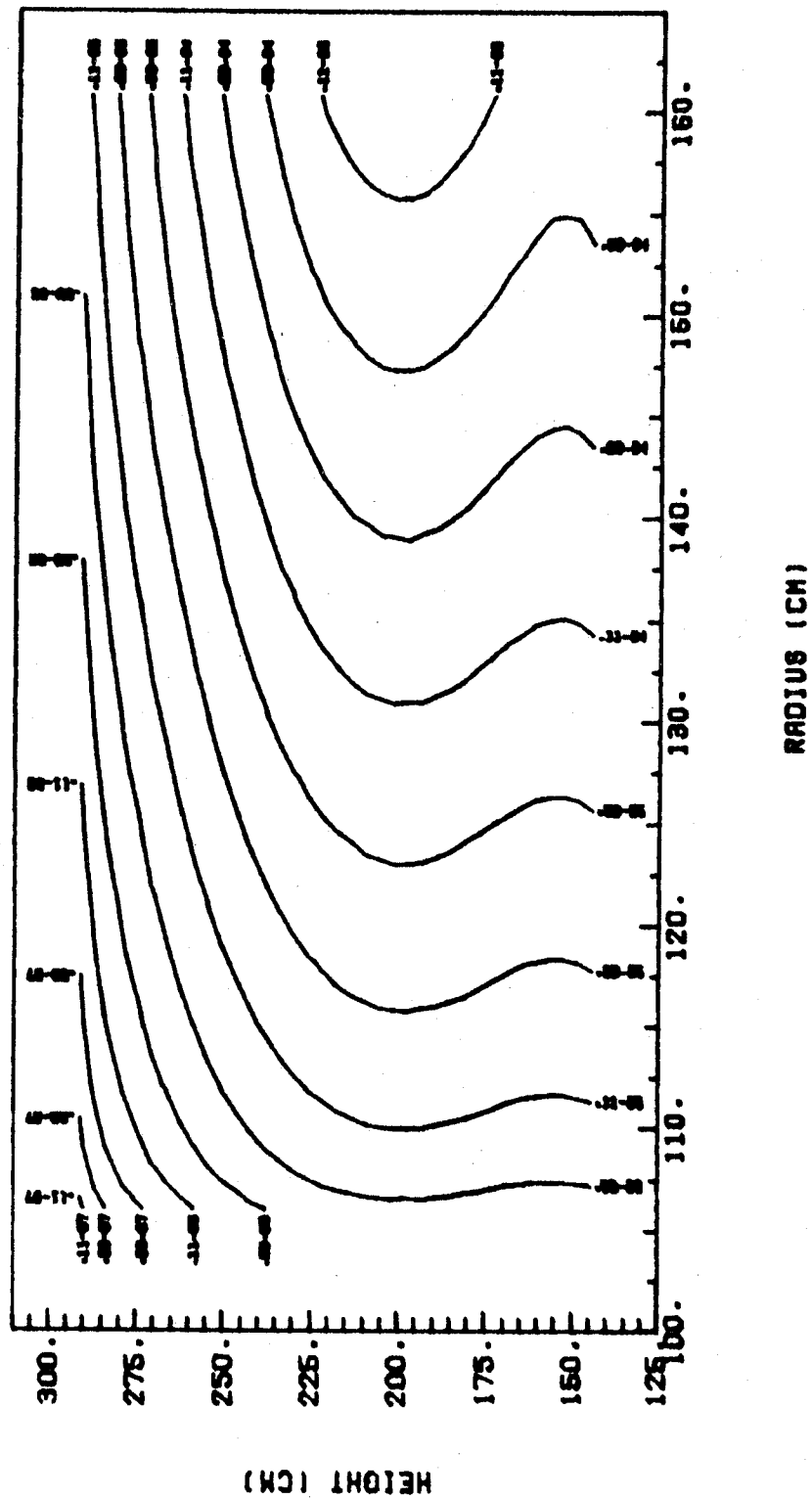


FIGURE 4 HEAT DEPOSITION RATE IN THE TOROIDAL FIELD MAGNET (W/CM²)

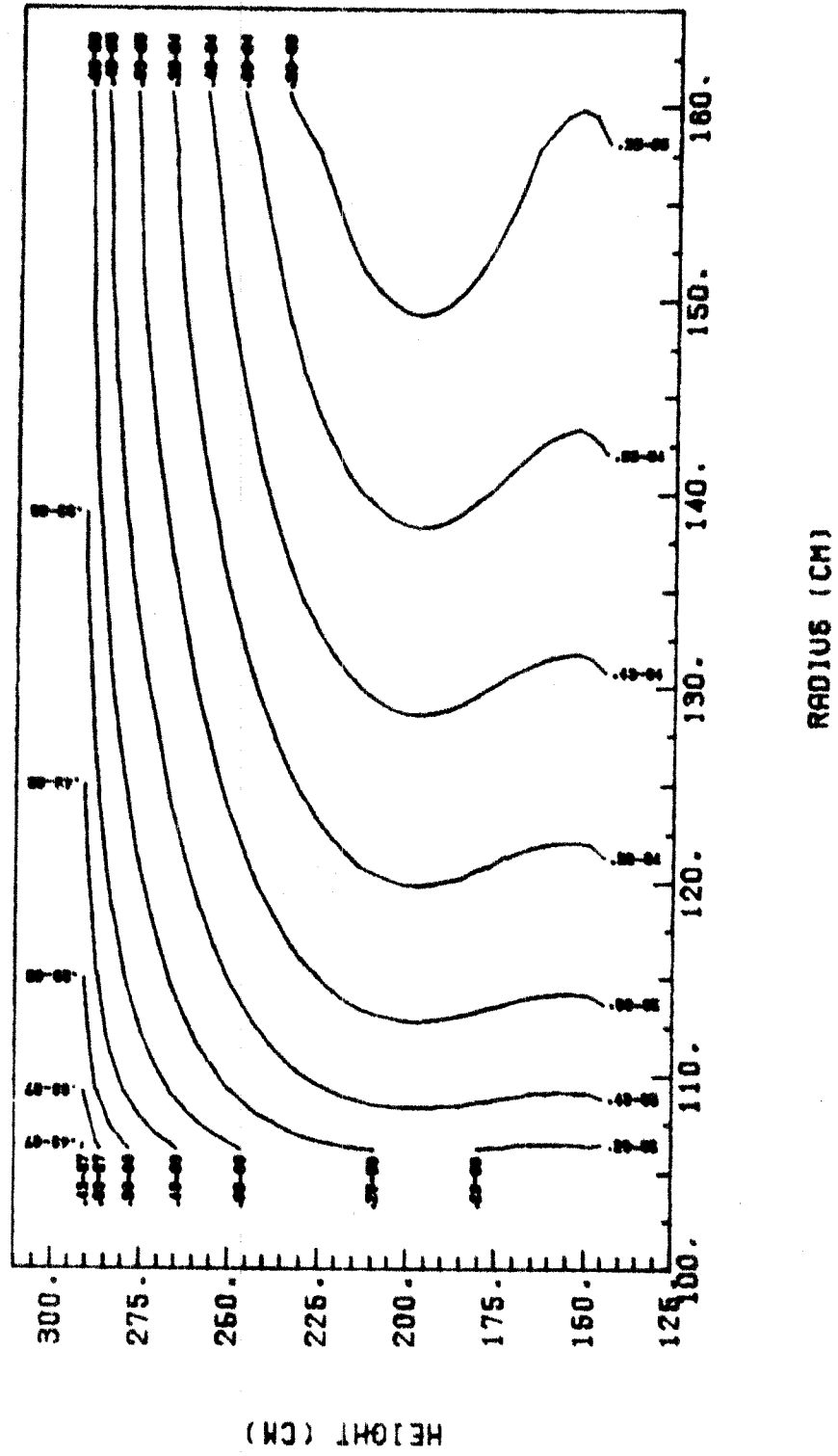


Figure (5) Heat Deposition Rate in the Cryosorption Panel

